RIS Optimal Element Selection for Enhanced Indoor Positioning Systems

Somayeh Bazin, Keivan Navaie
School of Computing and Communication
Lancaster University, Lancaster, UK
{s.bazin, k.navaie}@lancaster.ac.uk

***Abstract*—This paper proposes the use of Reconfigurable Intelligent Surfaces (RIS) to customize the Received Signal Strength (RSS) distribution in an indoor environment for an Indoor Positioning System (IPS). RIS is a promising technology that can improve wireless communication by manipulating the propagation of electromagnetic waves. Considering RSS distribution as an essential factor that directly affects the accuracy and reliability of indoor location estimation, in this study, we propose a novel IPS architecture that incorporates RIS as an intermediate layer to control the signal propagation between the transmitter and receiver. Then, intelligently search for RIS elements that can directly and freely change the RSS value in any particular positioning of the environment. Consequently, any arbitrary distribution of the RSS and radio map can be customized in an indoor environment without requiring RIS to change its configuration in time slots in order to support multi-users. By designing a radio map of an indoor environment, RIS can improve the accuracy and reliability of IPS, making it a valuable technology for various applications such as indoor navigation, asset tracking, smart building applications, and indoor augmented reality.**

***Index Terms*—Indoor positioning systems, Reconfigurable intelligent surface, Received signal strength.**

I. Introduction

Recently, there has been a significant surge in demand for location-based services. This is owing to their substantial contribution towards enhancing human life via many applications including safety and security, as well as market and health monitoring. This is because tracking and localizing targets are crucial in providing users with a comprehensive understanding of their surroundings. Nevertheless, providing localization services in an indoor environment presents significant challenges due to obstacles and abundant multipath. This ultimately results in poor performance with traditional positioning methods like Global Positioning Systems (GPS).

The Indoor Positioning System (IPS) has been developed to solve the positioning challenge in indoor environments. Various techniques, such as WiFi, Bluetooth, Zigbee, and Radio Frequency Identification (RFID), are employed for IPS [1], [2]. Among these methods, the Received Signal Strength (RSS) fingerprinting technique has gained widespread use due to its lower complexity, and ease of implementation, requiring no additional hardware.

In the RSS fingerprinting-based approach, a radio map of the target area is surveyed beforehand as a fingerprint during the offline phase. Subsequently, during the online phase, the algorithm searches for the best match of the already measured RSS values in the database [3].

Despite the popularity of the RSS technique, it is susceptible to high variability due to environmental dynamics which induces temporal fluctuation of RSS at a stationary receiver. Therefore, a mismatch between the pre-stored fingerprint and measured RSS in the same location degrades the RSS-based IPS accuracy.

To address the above issues, recent research has focused on exploring innovative IPS that incorporate Re-configurable Intelligent Surfaces (RIS) to address the challenge of accuracy improvement [4], [5], [6]. RIS offers the ability to customize signal propagation in an indoor environment by utilizing many low-cost passive units that can be easily reconfigured. The unique properties of RIS, enable IPS to alternate the radio map and manipulate multipath signals to improve localization accuracy.

Studies such as [7] and [8] demonstrated the potential accuracy improvement of RIS-enabled IPS through customizing RSS distribution. In their studies the favorable RSS distributions created by the RIS allow for improved differentiation of users located in different areas of the indoor environment. However, the main drawback of these studies is that they cannot customize the favorable RSS distribution for different users simultaneously. To address this issue, Time Division Multiplexing (TDM) is utilized to reconfigure RIS for each user in the time domain.

This paper presents a novel approach for customizing RSS distribution in an indoor environment for IPS. The proposed method utilizes RP-dependant RIS settings, which change the RIS configuration for different RPs, without the need to re-configure RIS. We introduce an optimal element selection methodology and demonstrate that there exists an element in the RIS that, by adjusting a phase shift, can freely change its amplitude to reach a desired signal strength at an RP, without affecting other lRPs. This enables multi-user support with only one RIS configuration, one access point, and relatively fewer activated RIS elements. The effectiveness of our proposed method is further demonstrated through simulations.

II. System Model and Proposed Methodology

This section presents the system model and RIS optimal selection algorithm. In typical indoor environments, the transmitted signal travels to the receiver through multiple

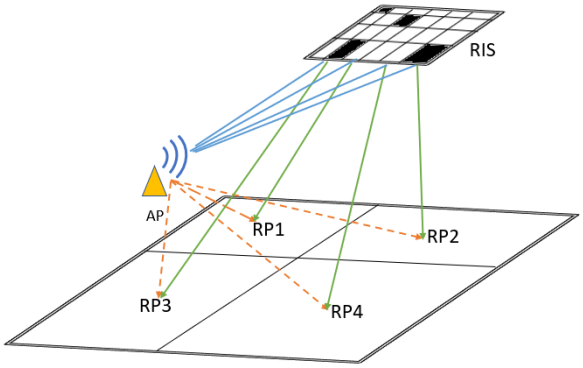

Fig. 1. Schematic of the proposed RIS incorporated signal propagation.

paths. However, with the incorporation of RIS in signal propagation, customized phase-shifted and gain-adjusted versions of the original signal also propagate through the paths from the Access Point (AP) to the RIS elements and ultimately from the RIS elements to the receiver, as shown in Fig. 1.

Let the RIS be composed of M elements, where $\mathbf{\Gamma} = [\Gamma_1, \Gamma_2, ..., \Gamma_M]$ and $\Gamma_m = r_m e^{-j\phi_m}$, represent the vector of the reflection coefficient of the RIS. Also, suppose the multipath channel consists of $I-1$ reflection paths and one Line of Sight (LoS) path from an AP to a RP. The indoor environment is divided into N RPs.Hence, the channel frequency response for the n-th RP can be represented as

$$H_n = \sum_{i=1}^{I} h_m(i,n) + \sum_{m=1}^{M} h_r(\Gamma_m, n), \tag{1}$$

where $\sum_{i=1}^{I} h_m(i,n)$ denotes the channel response from AP to RP including LoS and multipath, and $\sum_{m=1}^{M} h_r(\Gamma_m, n)$ represents RIS incorporated channel response including LoS from AP to RIS elements and LoS of RIS elements to RP. Thus,

$$h_m(i,n) = \frac{\lambda}{4\pi}.\frac{\sqrt{g_n^t g_n^r}.e^{-j2\pi d_m(i,n)/\lambda}}{d_m(i,n)}, \tag{2}$$

$$h_r(\Gamma_m, n) = \frac{\lambda}{4\pi}.\frac{\sqrt{g_m^t g_{m,n}^r}.\Gamma_m.e^{-j2\pi(d_r(m)+d_r(m,n))/\lambda}}{d_r(m)d_r(m,n)}, \tag{3}$$

where λ is the wavelength of the transmitted signal, $d_m(i,n)$ is the distances between AP and RP through different reflection paths, $d_r(m)$ and $d_r(m,n)$ are distances from AP to m-th RIS and distance between this element to n-th RP, respectively. Furthermore, g^t and g^r represent the power gain of the transmitter and receiver. The mean RSS at n-th RP block is [7]:

$$\overline{\text{RSS}}_{n,\mathbf{\Gamma}} = P_t + 20\log_{10}\left|h_m(i,n) + h_r(\Gamma_m, n)\right| + \xi, \tag{4}$$

where P_t is the transmitter signal power and ξ is the log-normal shadowing component which follows a Gaussian distribution with zero mean and variance of σ^2, $\mathcal{N}(0, \sigma^2)$. Equivalently, the RSS observed at the n-th RP is

$$\text{RSS}_{t,n,\mathbf{\Gamma}} = P_t + 20\log_{10}\left|\sum_{\rho=1}^{p} \alpha_{\rho,n}\delta(t-\tau_{\rho,n})\right|^2 + \xi, \tag{5}$$

where $p = I + M$ and $\alpha_{\rho,n}$ and $\tau_{\rho,n}$ are

$$\alpha_{\rho,n} = \begin{cases} \frac{\lambda}{4\pi}.\frac{\sqrt{g_n^t g_n^r}}{d_m(\rho,n)}, & \text{if } 1 \le \rho \le I, \\ \frac{\lambda}{4\pi}.\frac{\sqrt{g_m^t g_{m,n}^r}.r_\rho}{d_r(\rho)d_r(\rho,n)} & \text{if} I+1 \le \rho \le p. \end{cases}, \tag{6}$$

$$\tau_{\rho,n} = \begin{cases} \frac{d_m(\rho,n)}{C}, & \text{if } 1 \le \rho \le I, \\ \frac{d_r(\rho)+d_r(\rho,n)}{C} + \frac{\phi_\rho}{\omega} & \text{if} I+1 \le \rho \le p. \end{cases}, \tag{7}$$

and C is the speed of light and ω is the angular frequency of the signal. Furthermore, in (5)

$$\left|\sum_{\rho=1}^{p} \alpha_{\rho,n}\delta(t-\tau_{\rho,n})\right|^2 = \sum_{\rho=1}^{p} |\alpha_{\rho,n}|^2 \delta(t-\tau_{\rho,n}). \tag{8}$$

We define measured RSS as the average RSS value over the measurement time span $(t_1 : t_2)$. Therefore,

$$\text{RSS}_{n,\mathbf{\Gamma}} = P_t + 20\log_{10}\int_{t_1}^{t_2}\sum_{\rho=1}^{p} |\alpha_{\rho,n}|^2 \delta(t-\tau_{\rho,n})dt + \xi, \tag{9}$$

$$= P_t + 20\log_{10}\sum_{\rho=1}^{p} |\alpha_{\rho,n}|^2 \int_{t_1}^{t_2} \delta(t-\tau_{\rho,n})dt + \xi.$$

Equivalently, we can write

$$\sum_{\rho=I+1}^{p} |\alpha_{\rho,n}|^2 \int_{t_1}^{t_2} \delta(t-\tau_{\rho,n}) = 10^{\frac{\text{RSS}_{n,\mathbf{\Gamma}}-P_t}{20}} - \sum_{\rho=1}^{I} |\alpha_{\rho,n}|^2 \int_{t_1}^{t_2} \delta(t-\tau_{\rho,n}). \tag{10}$$

Here we assume that the difference in amplitude caused by the distance among RIS elements is negligible. Thus, we can represent $\alpha_{\rho,n}$ as $\alpha_{\rho,n} = b_n.r_\rho$. Additionally, suppose that there is a specific target value for RSS that we aim to measure at the n-th RP. This target value is chosen to minimize the positioning error at that RP. By substituting this target value in $\text{RSS}_{n,\mathbf{\Gamma}}$, (10) is rewritten as:

$$\sum_{\rho=I+1}^{p} |r_\rho|^2 \int_{t_1}^{t_2} \delta(t-\tau_{\rho,n}) = c_n. \tag{11}$$

The equation (11), shows that only the channels determine the RSS value at the n-th RP, where the corresponding channel's delay satisfies $t_1 \le \tau_{\rho,n} \le t_2$. Customizing a suitable radio map for all RPs can be therefore achieved by solving the following matrix equation:

$$\mathbf{\Delta}.\mathbf{r} = \mathbf{c}, \tag{12}$$

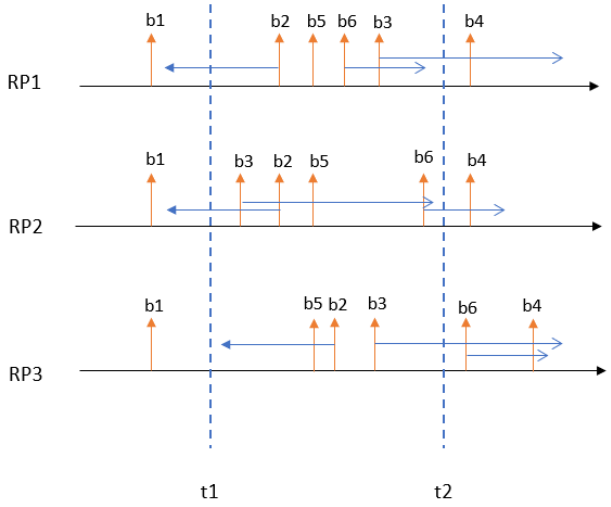

Fig. 2. (a): Channel frequency response before optimal element selection

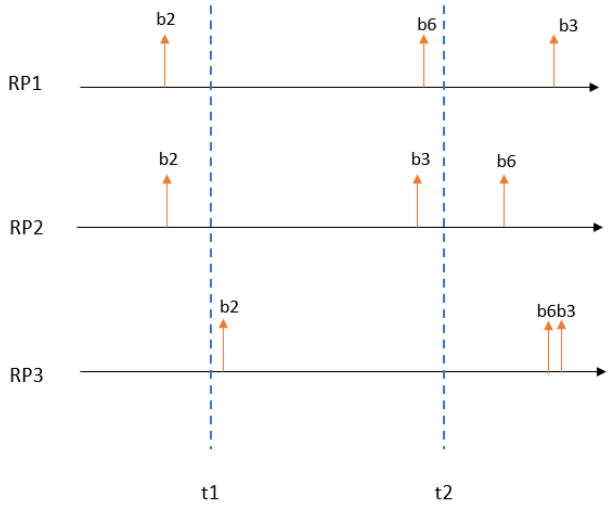

Fig. 3. (a): Channel frequency response after optimal element selection.

where $\mathbf{\Delta}$ is a $N \times M$ matrix including binary values of 0 and 1, $\mathbf{r}$ is a $M \times 1$ vector including the square amplitude coefficients of RIS, and $\mathbf{c}$ is a $N \times 1$ vector including the targeted RSS values at N RPs. Thus, for a desirable radio map, the objective is to determine $\mathbf{r}$ coefficients such that

$$\mathbf{r} = \mathbf{\Delta}^{-1}\mathbf{c}. \tag{13}$$

To solve (13), the following two conditions must be met. First, the matrix determinant, det($\mathbf{\Delta}$), must not equal zero. Second, only the positive solutions of $\mathbf{r}$ are acceptable.

While changing the phase shift of RIS can result in different values of $\mathbf{\Delta}$, it is not an efficient solution to search among all possible values of $\mathbf{\Delta}$ that satisfy these conditions. Therefore, we utilize a novel algorithm to solve (13).

In our approach, we use the optimal element selection of RIS. where N elements are selected out of total M elements for which the amplitude coefficients can assign any favorable radio map to an environment.

Suppose $\mathbf{T} = [\boldsymbol{\tau}_1^T, \boldsymbol{\tau}_2^T, ..., \boldsymbol{\tau}_M^T]$, where $\boldsymbol{\tau}_m = [\tau_{m,1}, \tau_{m,2}, ..., \tau_{m,N}]$. Clearly, before adjusting the phase shift of RIS $\tau_{m,n}$ corresponds to $(d_r(m) + d_r(m,n))/C$.

Lemma: Given a sufficiently large M relative to N, the RIS phase shift can be adjusted so that (12) can be written as

$$\mathrm{I}_N \times \dot{\mathbf{r}} = \mathbf{c}, \tag{14}$$

where I_N is the identity matrix of size N, $\dot{\mathbf{r}}$ is an N-dimensional vector selected from $\mathbf{r}$ based on the conditions of $\mathbf{\Psi}$, and $\mathbf{\Psi}$ is a vector of time shifts satisfying the following conditions: (i) its length is N, (ii) it includes either a unique maximum or minimum of $\boldsymbol{\tau}_m^T$ for $m = 1 : M$ and (iii) its members are mutually exclusive in their indexes. Specifically, if $\tau_{1,2}$ is the minimum or maximum of $\boldsymbol{\tau}_1$ and is a member of $\mathbf{\Psi}$, then $\tau_{2,2}$ cannot be selected if it is also the minimum of $\boldsymbol{\tau}_2$ since the index 2 is already included in $\mathbf{\Psi}$.

Proof: Assume $\min(\boldsymbol{\tau}_m) = \tau_{m,k}$ and $\tau_{m,k} \neq \tau_{m,n}$ for any $n = 1 : N, n \neq k$. Then we update $\mathbf{\Psi}$ to include $\tau_{m,k}$ and adjust ϕ_m so that

$$\tau_{m,k} + \phi_m/\omega = t_2 - \epsilon, \tag{15}$$

where ϵ is a small time shift less than the difference between the first and second minimum of $\boldsymbol{\tau_m}$ and it satisfies the following condition

$$\tau_{m,n} + \phi_m/\omega = \begin{cases} < t_2 & \text{if } n = k, \\ \geq t_2 & \text{if } n \neq k. \end{cases}, \tag{16}$$

similarly, if $\max(\boldsymbol{\tau}_m) = \tau_{m,k}$ and $\tau_{m,k} \neq \tau_{m,n}$ for any $n = 1 : N, n \neq k$. Then we can adjust ϕ_m so that

$$\tau_{m,k} + \phi_m/\omega = t_1 + \epsilon, \tag{17}$$

and

$$\tau_{m,n} + \phi_m/\omega = \begin{cases} \geq t_1 & \text{if } n = k, \\ < t_1 & \text{if } n \neq k. \end{cases}. \tag{18}$$

By adjusting the phase shift of ϕ_m as described earlier, the m-th element of the RIS can be used to determine the RSS of only the k-th RP. This element does not have any effect on any other RP in the environment. Therefore, a RIS element is obtained which is directly linked with a specific RP and its amplitude can be adjusted to set the desired RSS value without affecting other RPs. Similarly, we can find the associated RIS elements for any other RP. Once the associated element is identified, $\mathbf{\Psi}$ should be updated to include it.

After determining N associated elements of RIS, the rest $M - N$ elements' amplitude coefficient can be set to zero to prevent any possible interference caused by them. Consequently, $\mathbf{r}$ reduces to $\dot{\mathbf{r}}$ which only involves the determination of the amplitude of associated elements. Note that by applying the adjusted phase shift ϕ_m, (11) is simplified to

$$|r_m|^2 = c_k. \tag{19}$$

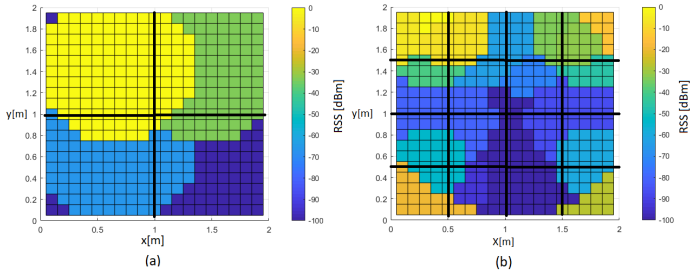

Fig. 4. The generated radiomap for the 2×2 environment: (a) $N = 4$, $M = 16$, RP size= $1 \times 1m^2$, (b) $N = 16$, $M = 64$, RP size= $0.5 \times 0.5m^2$,

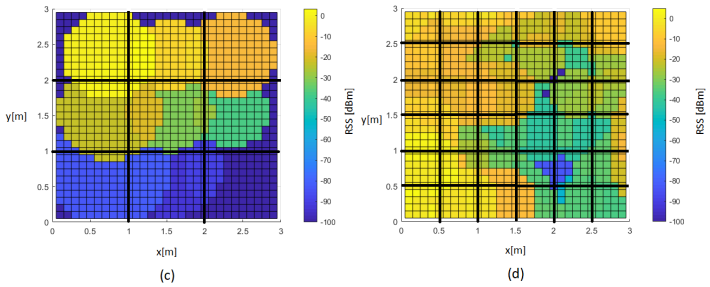

Fig. 5. The generated radiomap for the 3×3 environment: (a) $N = 9$, $M = 25$, RP size= $1 \times 1m^2$, (b) $N = 36$, $M = 100$, RP size= $0.5 \times 0.5m^2$,

Therefore, in the form of a matrix equation, (14) is obtained and the relative amplitude coefficient of m-th element can be achieved by solving (19).■

Optimal element selection for an environment with 3 RPs and a RIS of 6 elements is illustrated in Figs . 2 and 3. Fig. 2 depicts the frequency response of RIS in different RPs prior to the application of phase shift and optimal element selection. The optimal selection of elements is performed by choosing the sixth, third, and second RIS elements for the first, second, and third RP, respectively. The corresponding phase shift of each selected element is then determined, and the amplitude gain for the remaining elements is set to zero. Resulting in the frequency response as in Fig. 3.

III. RESULTS AND DISCUSSIONS

In this section, we present the results of the implementation of our proposed optimal element section algorithm. We considered square rooms of size 2m $\times$ 2m and 3m $\times$ 3m as our experimental indoor environments where it is divided into a different number of RPs and each RP is assigned a unique value in the range of -100 dBm: 0 dBm as its RSS. The left corner of the room is considered to be the origin $(0, 0, 0)$ in the xyz plane, and the AP is located at the center of the room. Six multi-path signals reflected from the four side walls, the roof, and the floor of the environment are considered in addition to the Line of Sight (LoS) signal. The RIS is positioned on the plane at a height of $z = 3$ units, which is the height of the room's roof. The center of the RIS is also located at the center of the room, the distance between the center of RIS neighbor elements is 0.2 m. The carrier frequency of the wireless signal is 2.4 GHz. Each RP covers a square area in the environment

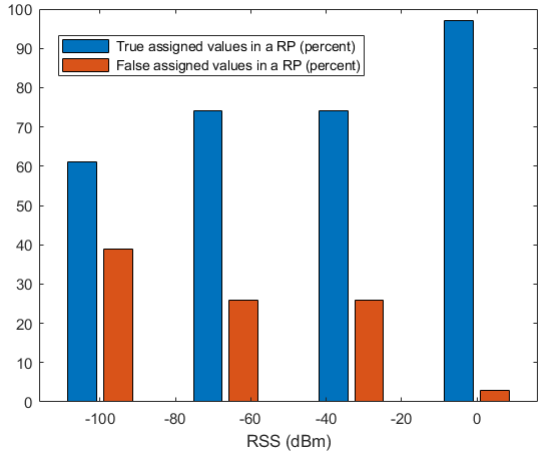

Fig. 6. Histogram of true and false RSS assignments within an RP for $N = 4$, $M = 16$, RP size= $1 \times 1m^2$

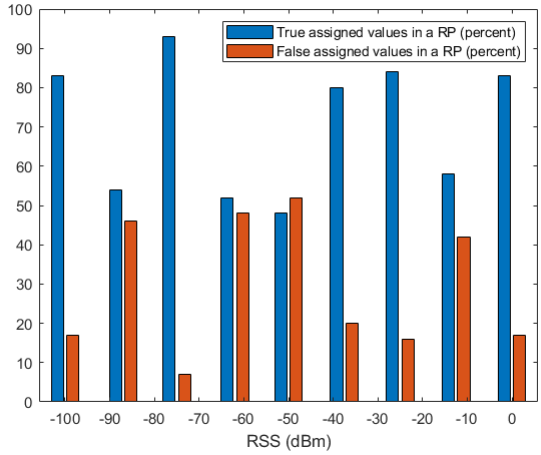

Fig. 7. Histogram of true and false RSS assignments within an RP for $N = 9$, $M = 25$, RP size= $1 \times 1m^2$.

where the center of an RP is assigned the corresponding RSS value. The size of the RP can vary.

Figs. 4 and 5 show the results obtained by applying the proposed algorithm in two different indoor environments with sizes of 2m $\times$ 2m and 3m $\times$ 3m, respectively. The radio map and the RP sizes are changed to investigate the impact of these parameters. The solid black lines represent the borders of the RPs. While most of the RP area has the assigned target RSS, some regions within an RP may have different values. The presence of interference from neighboring RPs can lead to the variation of RSS inside an RP. These conditions are primarily caused by the relative physical positioning of the RIS elements and the RPs.

Figs. 6 and 7 show the histograms of the total true assigned regions compared to the false assigned regions within different RPs under two different settings. These results confirm that, for the most part, the RPs are occupied by their assigned RSS values.

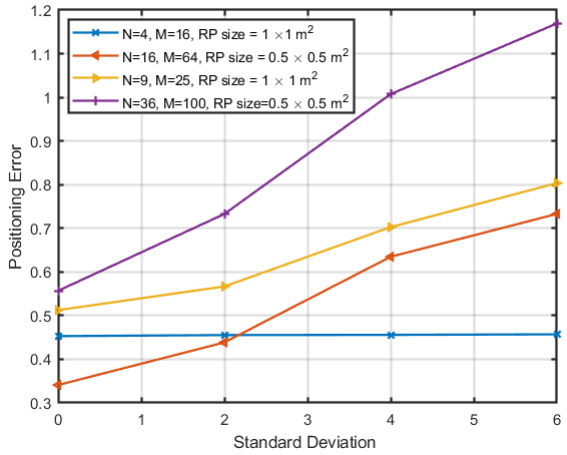

Fig. 8. Comparison of the positioning error of customized radio map generated in different settings versus standard deviation of RSS.

In Fig. 8, we compare the localization error of indoor environments under different settings, as demonstrated in Figs .4 and 5, for various standard deviations of RSS. The localization error is calculated using multiple runs of the following equation:

$$P_e = \frac{1}{H} \sum_{h \in H} |p_h^e - p_h^g| \,, \tag{20}$$

where the user's position changes randomly, p_h^e represents the estimated position, and p_h^g represents the ground truth. While this simulation confirms appropriate positioning accuracy, it is worth noting that as the size of the RPs decreases, the probability of neighboring RSS leakage to the closed RPs increases, thereby reducing the accuracy of the localization system.

IV. Conclusion

This paper proposes an optimal element selection method for the RIS to customize the RSS values in an indoor environment. The study demonstrates that any arbitrary RSS distribution can be assigned to an environment as long as an associated RIS element can be found for each RP in the environment. The proposed method enables different settings of RIS to be applied for each RP, allowing multiple users to benefit from a customized RSS distribution without requiring the RIS to be reconfigured for each user. Finally, by utilizing customized RSS distribution in different RPs, high accuracy in positioning is achieved.

References

[1] Hameed *et al.*, "Survey on indoor positioning applications based on different technologies," in *2018 12th International Conference on Mathematics, Actuarial Science, Computer Science and Statistics (MACS)*, 2018, pp. 1–5.

[2] A. Yassin *et al.*, "Recent advances in indoor localization: A survey on theoretical approaches and applications," *IEEE Communications Surveys Tutorials*, vol. 19, no. 2, pp. 1327–1346, 2017.

[3] P. Bahl and V. Padmanabhan, "Radar: an in-building rf-based user location and tracking system," in *Proceedings IEEE INFOCOM 2000. Conference on Computer Communications. Nineteenth Annual Joint Conference of the IEEE Computer and Communications Societies (Cat. No.00CH37064)*, vol. 2, 2000, pp. 775–784 vol.2.

[4] T. Ma *et al.*, "Distributed reconfigurable intelligent surfaces assisted indoor positioning," *IEEE Transactions on Wireless Communications*, vol. 22, no. 1, pp. 47–58, 2023.

[5] T. Ma, Y. Xiao, X. Lei, W. Xiong, and Y. Ding, "Indoor localization with reconfigurable intelligent surface," *IEEE Communications Letters*, vol. 25, no. 1, pp. 161–165, 2021.

[6] Z. Yang *et al.*, "Wireless indoor simultaneous localization and mapping using reconfigurable intelligent surface," in *2021 IEEE Global Communications Conference (GLOBECOM)*, 2021, pp. 1–6.

[7] H. Zhang *et al.*, "Metalocalization: Reconfigurable intelligent surface aided multi-user wireless indoor localization," *IEEE Transactions on Wireless Communications*, vol. 20, no. 12, pp. 7743–7757, 2021.

[8] H. Zhang, H. Zhang, B. Di, K. Bian, Z. Han, and L. Song, "Towards ubiquitous positioning by leveraging reconfigurable intelligent surface," *IEEE Communications Letters*, vol. 25, no. 1, pp. 284–288, 2021.